Formation of the Galactic bulge from a two-component stellar disk: Explaining cylindrical rotation and vertical metallicity gradient

Kenji Bekki¹[⋆] and Takuji Tsujimoto²

- ¹ICRAR M468 The University of Western Australia 35 Stirling Hwy, Crawley Western Australia, 6009
- National Astronomical Observatory, Mitaka-shi, Tokyo 181-8588, Japan

Accepted, Received 2005 February 20; in original form

ABSTRACT

Recent observational studies have revealed that the Galactic bulge has cylindrical rotation and a steeper vertical metallicity gradient. We adopt two representative models for the bulge formation and thereby investigate whether the two models can explain both the observed cylindrical rotation and vertical metallicity gradient in a self-consistent manner. One is the "pure disk scenario" (PDS) in which the bulge is formed from a pure thin stellar disk through spontaneous bar instability. The other is the "two-component disk scenario" (TCDS) in which the bulge is formed from a disk composed of thin and thick disks through bar instability. Our numerical simulations show that although PDS can reproduce the cylindrical rotation, it shows a rather flatter vertical metallicity gradient that is inconsistent with observations. The derived flatter metallicity gradient is due to the vertical mixing of stars with different initial metallicities by the stellar bar. This result implies that the bulge can not be simply formed from a pure thin stellar disk. On the other hand, the bulge formed from the two-component disk in TCDS can explain both the observed cylindrical rotation and vertical metallicity gradient of the Galactic bulge reasonably well. In TCDS, more metal-poor stars at higher |z| (vertical distance) which originate from the already dynamically hotter thick disk can not be strongly influenced by vertical mixing of the bar so that they can stay in situ for longer timescales and thus keep the lower metallicity at higher |z|. Consequently, the vertical metallicity gradient of the bulge composed of initially thin and thick disk stars can not be so flattened, even if the gradient of the thin disk can be flattened significantly by the bar in TCDS. We therefore suggest that a significant fraction of the present Galactic bulge is composed of stars initially in the inner part of the thick disk and thus that these bulge stars and the thick disk have a common origin. We also suggest that the Galaxy might well have experienced some merger events that could dynamically heat up its inner regions until ~ 10 Gyr ago.

 \mathbf{Key} words: The Galaxy:formation – The Galaxy:bulge – The Galaxy:disk – The Galaxy:evolution

1 INTRODUCTION

The Galaxy is observed to have a "boxy" bulge in near-infrared images (Dwek et al. 1995) and the nature and the origin of the inner triaxial shape of the Galaxy (i.e., bar/bulge) has been extensively discussed by several authors (e.g., Babusiaux & Gilmore 2005; Rattenbury et al. 2007). Recent spectroscopic observations on stellar abundances and

kinematics of the Galactic bulge have provided new clues to the origin of the triaxial bulge (e.g., Meléndez et al. 2008; Zoccali et al. 2008; Babusiaux et al. 2010). Meléndez et al. (2008) found no/little differences in chemical abundances of stars between the Galactic bulge and the thick disk and accordingly suggested a similar chemical evolution history between the two components of the Galaxy (see also Ryde et al. 2010, Alves-Brito et al. 2010). Zocalli et al. (2008) found a steep metallicity gradient along the minor axis of the bulge and suggested that the presence of the vertical

metallicity gradient is consistent with dissipative processes of the bulge formation. Babusiaux et al. (2010) revealed that (i) the bulge has two distinct populations and (i) the metalrich population has bar-like kinematics whereas the metalpoor one has kinematics similar to those of an old spheroid or a thick disk (see also de Propris et al. 2011).

Combes & Sanders (1981) first pointed out that galactic bars can be identified as boxy/peanut bulges in the edgeon view. Dynamical models in which the Galactic bulge is
formed from the thin disk through spontaneous bar instability have been successfully constructed (e.g., Fux 1997) and
used to discuss the bulge formation in the context of PDS.
Although this PDS can explain consistently the observed
cylindrical rotation and velocity dispersion profiles of stars
in the Galactic bulge (e.g., Howard et al. 2009; Shen et al.
2010), recent observational studies have suggested that the
observed vertical metallicity gradient of the bulge can not
be so simply explained by the PDS (e.g., Minniti et al. 1995;
Zoccali et al. 2008; Babusiaux et al. 2010): evolution of the
vertical metallicity gradient however has not been extensively investigated by theoretical studies.

The purpose of this paper is thus to adopt PDS and thereby to investigate the evolution of the vertical metallicity gradient of the Galactic bulge formed from a pure thin stellar disk through bar instability based on collisionless N-body numerical simulations. We also adopt TCDS and thereby investigate whether the simulated bulge can explain both the observed cylindrical rotation and the vertical metallicity gradient in a self-consistent manner. Given that the Galaxy is observed to have the thick disk as well as the thin one (e.g., Gilmore & Reid 1983), it is natural to adopt a two-component disk model for discussing the origin of the bulge.

2 THE MODELS

2.1 PDS

The Galaxy in PDS is modeled as a bulge-less disk galaxy with the total mass $M_{\rm d}$ and size $R_{\rm d}$ embedded in a massive dark matter halo. The total mass and the virial radius of the dark matter halo of the disk are denoted as $M_{\rm dm}$ (= $f_{\rm dm}M_{\rm d}$, where $f_{\rm dm}$ is the mass-ratio of dark matter to disk) and $r_{\rm vir}$, respectively. We adopted an NFW halo density distribution (Navarro, Frenk & White 1996) suggested from CDM simulations:

$$\rho(r) = \frac{\rho_0}{(r/r_s)(1 + r/r_s)^2},\tag{1}$$

where r, ρ_0 , and $r_{\rm s}$ are the spherical radius, the characteristic density of a dark halo, and the scale length of the halo, respectively. The c parameter (= $r_{\rm vir}/r_{\rm s}$) is set to be 12 in the present study.

The stellar component of the disk is assumed to have an exponential profile with a radial scale length (a) and a vertical scale height (h). In addition to the rotational velocity made by the gravitational field of disk and halo component, the initial radial and azimuthal velocity dispersion are given to the disk component according to the epicyclic theory with Toomre's parameter (Binney & Tremaine 1987) Q=1.5. The vertical velocity dispersion at a given radius is set to be 0.5 times as large as the radial velocity dispersion at that

point. Although we have investigated different models with different parameters, we describe the results of the model "PDS1" with $f_{\rm dm}=15.7$, $r_{\rm vir}=9R_{\rm d}$, $M_{\rm d}=4\times10^{10}M_{\odot}$, $R_{\rm d}=17.5$ kpc, a=1.75 kpc, and h=0.35 kpc in the present study, because this model clearly shows a bar (=boxy bulge) with the cylindrical rotation consistent with the observed one.

2.2 TCDS

Since our recent paper (Bekki & Tsujimoto 2011) has already described the methods and techniques to construct two-component stellar disk models in detail, we briefly describe the models here. The Galaxy consists of the following two stellar components in TCDS. One is a thick disk (or a very flattened spheroid supported largely by rotation) that was formed as the first thin stellar disk (FD) and later dynamically heated up by merger events. The other is a thin disk (or second disk, SD) that was later formed via gas accretion from the Galactic halo after the formation of the thick disk. These dynamically hot and cold stellar disks can be transformed into a bar (boxy bulge) through bar instability in TCDS. The initial structural and kinematical properties of the stellar disk and the dark matter halo in FD and SD are essentially the same as those of the pure stellar disk adopted for PDS. The mass $(M_{d,1})$, size $(R_{d,1})$, scale-length (a_1) , and scale-hight (h_1) of the initial exponential disk and the mass $(M_{dm,1})$, virial radius $(r_{vir,1})$, and c-parameter (c_1) of the dark matter halo in FD are $8 \times 10^9 M_{\odot}$, 17.5 kpc, 1.75 kpc, 350 pc, $6.3 \times 10^{11} \mathrm{M}_{\odot}$, 210 kpc, and 12, respectively.

The initial disk merges with a dwarf disk galaxy so that a thick disk can be formed within ~ 40 dynamical timescale $(t_{\rm dyn})$ of the initial disk (Bekki & Tsujimoto 2011). The initial disk and the dwarf are assumed to have self-similar structural and kinematical properties of stellar disks and dark matter halos. The disk size of the dwarf $(R_{d,dw})$ is assumed to depend on the mass of the disk $(M_{d,dw})$ such as $R_{\rm d,dw} \propto M_{\rm d,dw}^{0.5}$, which corresponds to the Freeman's law (Freeman 1970). Therefore, the mass-ratio (m_2) of the dwarf to FD can determine the size of the stellar disk for the dwarf and thus the structural and kinematical properties of the dark matter halo and the stellar disk. The stellar remnant of a minor merger with $m_2 = 0.2$, orbital inclination angles of 30°, orbital eccentricities of 0.5, and pericenter distances of $R_{\rm d,1}$ (=17.5 kpc) are used as the thick disk in the present study. After the thick disk formation, SD is assume to grow slowly for $20t_{\rm dyn}$ while the thick disk and the dark matter halo can dynamically response to the growing SD. The mass $(M_{d,2})$, size $(R_{d,2})$, scale-length (a_2) , and scale-hight (h_2) of the exponential stellar disk (SD) are $4 \times 10^{10} M_{\odot}$, 17.5 kpc, 3.5 kpc, and 350 pc, respectively. The two-component disk constructed above is referred to as the "TCDS1" model.

2.3 Radial and vertical metallicity gradients

We adopt the same model for the radial metallicity gradient of a stellar disk in PDS and TCDS as that used in Bekki & Tsujimoto (2011). We consider that the metallicity gradient is different between inner $(R < R_{\rm b})$ and outer $(R \geqslant R_{\rm b})$ regions of FD and SD, where $R_{\rm b}$ is set to be 2 kpc corresponding to the size of the bulge. We allocate metallicity to

each disk star in the outer disk $(R \ge R_b)$ according to its initial position: the metallicity of the star at r = R (kpc) is given as:

$$[m/H]_{r=R} = [m/H]_{d,r=0} + \alpha_d \times R.$$
 (2)

The constant $[\mathrm{m/H}]_{\mathrm{d,r=0}}$ is determined such that the metallicity at the solar radius $(R=R_{\odot} \text{ corresponding to 8.5 kpc})$ is consistent with the observed one for a given α_{d} . We adopt the observed value of $\alpha_{\mathrm{d}} \sim -0.04$ (e.g., Andrievsky et al. 2004). In PDS, $[\mathrm{m/H}]_{\mathrm{d,r=0}}$ is set to be 0.14 for $\alpha_{\mathrm{d}} \sim -0.04$ so that the mean metallicity at $R=R_{\odot}$ can be -0.2. In TCDS, $[\mathrm{m/H}]_{\mathrm{d,r=0}}$ is set to be -0.36 (0.14) for FD (SD) for $\alpha_{\mathrm{d}} \sim -0.04$ so that the mean metallicity at $R=R_{\odot}$ can be -0.7 (-0.2). The dwarf has $\alpha_{\mathrm{d}}=-0.04$ and $[\mathrm{m/H}]_{\mathrm{d,r=0}}=-0.54$ so that the metallicity of the dwarf (-0.18 dex lower than FD) is consistent with the luminosity-metallicity relation of galaxies ($M \propto Z^{0.4}$; Mould 1984).

We assign the metallicity of a star at r = R in the inner disk $(R < R_b)$, where r(R) is the projected distance (in units of kpc) of the star from the center of the disk, to be:

$$[m/H]_{b,r=R} = [m/H]_{b,r=0} + \alpha_b \times R.$$
 (3)

We consider that the slope of the metallicity gradient is a free parameter and investigate different models with different $\alpha_{\rm b}$. The central metallicity of the disk is determined such that the metallicity at $R=R_{\rm b}$ is consistent with the one derived from the above equation (2). For example, if we adopt $\alpha_{\rm b}=-0.4$ for FD in TCDS, then $[{\rm m/H}]_{\rm b,r=0}=0.36$ for $\alpha_{\rm d}=-0.04$ and $[{\rm m/H}]_{\rm d,r=0}=-0.36$. The inner radial metallicity gradients for initial disks in PDS and TCDS are denoted as $\alpha_{\rm b,pds}$ and $\alpha_{\rm b,tcds}$, respectively.

The initial metallicity of a star with r=R and a vertical distance (|z|) from the x-y (equatorial) plane of the Galaxy depends also on |z| and it is assigned to be as follows

$$[m/H]_{r=R,|z|} = [m/H]_{|z|=0} + \alpha_v \times |z|,$$
 (4)

where [m/H]_{r=R,|z|=0} is a metallicity at r=R and |z|=0. Although $\alpha_{\rm v}\approx -0.4$ could be reasonable (Frogel et al. 2000), we investigate models with different $\alpha_{\rm v}$. The slope $\alpha_{\rm v}$ is denoted as $\alpha_{\rm v,pds}$ and $\alpha_{\rm v,tcds}$ for PDS and TCDS, respectively.

Using the latest version of GRAPE (GRavity PipE, GRAPE-DR) – which is the special-purpose computer for gravitational dynamics (Sugimoto et al. 1990), we run N-body simulations of the dynamical evolution of stellar disks for $16-20t_{\rm dyn}$ (2.8-3.5 Gyr) during which stellar bars can be fully developed. We investigate rotational velocities (V_{ϕ}) at different |z| and vertical metallicity gradients for the bulge regions at the final time step in models with different $\alpha_{\rm b,pds},\,\alpha_{\rm b,tcds},\,\alpha_{\rm v,pds}$ and $\alpha_{\rm v,tcds}$ both for PDS and TCDS. The total number of particles used for a model is 900000 in PDS and 1180000 in TCDS. The adopted gravitational softening length is fixed at $0.014R_{\rm d}$, which corresponds to 252pc for $R_{\rm d}=17.5$ kpc.

3 RESULTS

Fig. 1 shows that a strong stellar bar is fully developed by spontaneous bar/buckling instability in the central region of the stellar disk and the disk looks like a disk galaxy with a bulge in edge-on view for the model PDS1. As shown in

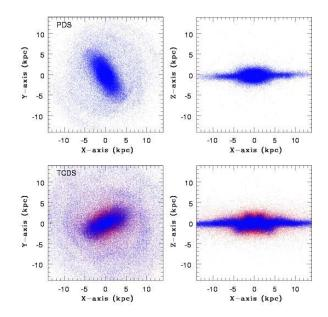


Figure 1. The final distributions of stars projected onto the x-y (left) and x-z planes (right) in the model PDS1 (upper two) and those in the model TCDS1 (lower two). The blue and red particles represent stars initially in the thin and thick disks, respectively, in the lower two panels.

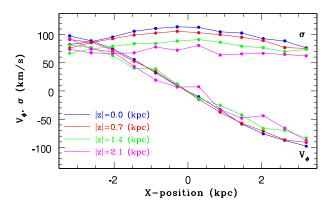


Figure 2. The rotational velocity (V_{ϕ}) and velocity dispersion (σ) along the x-axis of the simulated bulge (=bar) at different vertical distances (|z|) in the model PDS1: for |z| = 0 kpc (blue), 0.7 kpc (red), 1.4 kpc (green), and 2.1 kpc (magenta).

Fig. 2, the central region of the disk with R < 3 kpc clearly show rotation at different |z| ($0 \le |z| \le 2.1$ kpc), which demonstrates that the bulge has cylindrical rotation. The derived amplitude ($\sim 100 \text{ km s}^{-1}$) and profile of cylindrical rotation in this model are in good agreement with the latest observational results by Howard et al. (2009). The velocity dispersion (σ) can be larger than $\sim 100 \text{ km s}^{-1}$ in the center of the bar and depends on |z| such that σ is larger for smaller |z| in the bulge. These results are also in good agreement with the observations by Howard et al. (2009).

Fig. 3 shows how the initial vertical metallicity gradient of the stellar disk in PDS evolves as the stellar bar change radial and vertical stellar structures owing to its dynamical action on the disk. It is clear that irrespective of $\alpha_{\rm b,pds}$ and $\alpha_{\rm v,pds}$, the initial steep vertical gradient can become rather flattened within 3.5 Gyr. This is mainly because stellar pop-

4 K. Bekki and T. Tsujimoto

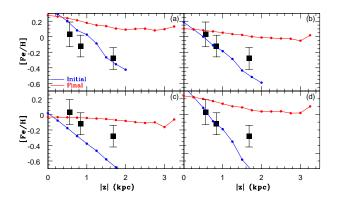


Figure 3. The initial (blue) and final (red) vertical metallicity gradients within the bulge region (R < 2 kpc) in the model PDS1 with different $\alpha_{\rm b,pds}$ and $\alpha_{\rm v,pds}$: (a) $\alpha_{\rm b,pds} = -0.4$ and $\alpha_{\rm v,pds} = -0.4$, (b) $\alpha_{\rm b,pds} = -0.2$ and $\alpha_{\rm v,pds} = -0.4$, (c) $\alpha_{\rm b,pds} = 0$ and $\alpha_{\rm v,pds} = -0.4$, and (d) $\alpha_{\rm b,pds} = -0.4$ and $\alpha_{\rm v,pds} = -0.6$. Three observational data points on mean metallicities and dispersions at |z| = 0.56 kpc, 0.84 kpc, and 1.68 kpc from Zoccali et al. (2008) are also shown by filled squares and error bars, respectively, in each frame for comparison.

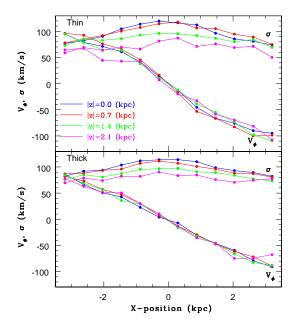


Figure 4. The same as Fig.2 but for the model TCDS1. Here V_{ϕ} and σ profiles are shown separately for the thin disk (upper) and the thick one (lower) for clarity.

ulations that are located at different |z| and thus have different [Fe/H] can be mixed well during the bar instability and the evolution of the bar. The simulated vertical metallicity gradients do not fit well with the observational results, in particular, for $|z| \sim 1.7$ kpc, which suggests that the bulge can not be simply formed from a pure thin one-component stellar disk through bar instability.

As shown in Fig. 1, a stellar bar can be developed in the two-component disk within ~ 2 Gyr in the model TCDS1 and it looks like a (boxy) bulge in edge-on view. Although

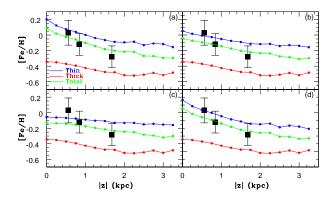


Figure 5. The same as Fig. 4 but for the final vertical metallicity gradients for the thin disk (blue), thick one (red), and total (green) in the model TCDS with different $\alpha_{\rm b,tcds}$ and $\alpha_{\rm v,tcds}$: (a) $\alpha_{\rm b,tcds} = -0.4$ and $\alpha_{\rm v,tcds} = -0.4$, (b) $\alpha_{\rm b,tcds} = -0.2$ and $\alpha_{\rm v,tcds} = -0.4$, (c) $\alpha_{\rm b,tcds} = 0$ and $\alpha_{\rm v,tcds} = -0.4$, and (d) $\alpha_{\rm b,tcds} = -0.4$ and $\alpha_{\rm v,tcds} = -0.6$.

the thick disk can not become a bar for itself owing to the smaller mass fraction of the disk, it can become a bar when the thin disk is transformed into a bar through bar instability. Fig. 4 clearly shows that both the thin and thick disks show the maximum V_{ϕ} of $\sim 100~\rm km~s^{-1}$ and have cylindrical rotation with the amplitudes and profiles similar to each other in the central 3 kpc. The simulated maximum value of σ and σ -profiles dependent on |z| in the thin and thick disks are in good agreement with the observed ones. Although the thick disk initially has higher velocity dispersions and a smaller amplitude of rotation than the thin disk, the two components can finally have similar kinematical properties: the thick disk has σ at |z|=1.4kpc and 2.1 kpc higher than those of the thin disk.

Fig. 5 shows that although the initial vertical metallicity gradient of the bulge region in the thin disk can be significantly flattened, the simulated profile for the whole disk can fit much better with the observational data in comparison with those derived in the PDS1. The most important reason for this is that the mean metallicity at |z| = 1.7kpc in this model can be as low as -0.2 owing to the presence of metal-poor stars of FD there: these metal-poor stars originate from R > 3 kpc of FD. Since these stars initially stay at higher |z| in the dynamically hotter thick disk, they can not be strongly influenced by the bar and consequently they can stay longer at higher |z| and thus can keep the lower mean metallicity there. As a result of this, the mean metallicity of the whole disk (bulge) at higher |z| can keep lower. In addition, the bar in this model does not mix so well stellar populations with different metallicities in the thin disk in comparison with the PDS1. This less efficient mixing of stellar populations with different initial |z| and [Fe/H]also contribute to the steeper vertical metallicity gradient to some extent. The results for three different models in Fig. 5 show that steeper vertical metallicity gradients can be seen in models with steeper $\alpha_{\rm b,tcds}$ in TCDS. Thus TCDS can reproduce reasonably well the cylindrical rotation and vertical metallicity gradient observed in the Galactic bulge in a self-consistent manner.

4 DISCUSSION

The results of the present numerical simulations suggest that if the Galactic bulge was formed from an initially thin stellar disk through bar instability, then the present bulge is unlikely to have a steep vertical metallicity gradient owing to the vertical mixing of stellar populations with different metallicities by the bar. However, it should be stressed here that the present study is based on collisionless N-body simulations that do not include gas dynamics which could possibly suppress the formation of strong bars. Accordingly it would overestimate the degree of the vertical mixing of stellar populations by stellar bars and thus can not completely rule out a possibility that dissipative gas dynamics can keep the original vertical metallicity gradient of the bulge.

In TCDS, FD was formed with a star formation time scale $t_{\rm sf}$ of ~ 1 Gyr about 10 Gyr ago through dissipative collapse or merging of subgalactic clumps. Such a short $t_{\rm sf}$ is suggested to be consistent with high $[\alpha/\text{Fe}]$ observed in the bulge, though $t_{\rm sf}$ could be ~ 0.1 Gyr (e.g., Ballero et al. 2007). Stars in the inner region of FS finally become the old population of the bulge whereas those in the outer one become the thick disk. After merger events about 10 Gyr ago, SD started to form and its inner part (< 2kpc) could form earlier and much more rapidly owing to its shorter dynamical time scale in comparison with the outer part. Stars in the inner part of SD can finally become relatively younger populations of the bulge compared with those in FD. Owing to a rapid time scale of star formation in the bulge composed of inner FD and SD stars, the chemical abundances of the old stellar populations in TCDS can be very similar to what our previous bulge formation model with a rapid star formation time scale predicted (Tsujimoto et al. 2010). The model by Tsujimoto et al. (2010) can explain the observed MDF (Fulbright et al 2006) and high $[\alpha/\text{Fe}]$ (Rich & Origlia 2005; Fulbright et al. 2007; Johnson et al. 2011) for the bulge: we thus suggest that the present TCDS is in good agreement with these observations. We will extensively investigate chemical abundances of the bulge using a fully consistent chemodynamical bulge model in our forthcoming papers.

The present TCDS suggests that the observed similarity in stellar populations between the bulge and the thick disk (e.g., Meléndez et al. 2008; Bensby et al. 2010) can be naturally explained in TCDS. Also, the simulated two-component bulge in the present study can explain the observed presence of two distinct populations with a varying mix of the two along the minor axis of the bulge (Babusiaux et al. 2010). Thus the Galaxy might well have experienced merger events about 10 Gyr ago, resulting in the transformation of a thin disk into either a thick disk or a flattened spheroid supported mainly by rotation.

Previous chemical evolution models showed that the IMF needs to be significantly flatter than the Salpeter one to explain the observed metallicity distribution function (MDF) and higher $[\alpha/\text{Fe}]$ of the bulge stars (e.g., Tsujimoto et al. 2010). On the other hand, such a flat IMF is not necessary to explain the observed chemical abundance of the thick disk stars around the solar neighborhood (e.g., Chiappini et al. 1997). In TCDS, the present bulge stars and thick disk ones around the solar neighborhood can originate largely from inner and outer regions of FD, respec-

tively. Therefore, the IMF in FD needs to depend on R such that it is flatter in the inner region of the Galaxy. This possible radial-dependent IMF of the Galaxy may well have some important implications on the Galaxy evolution.

5 ACKNOWLEDGMENT

We are grateful to the anonymous referee for valuable comments which contribute to improve the present paper.

REFERENCES

Alves-Brito, A., Meléndez, J., Asplund, M., Ramírez, I., Yong, D., 2010, A&A, 513, 35

Andrievsky, S. M., Luck, R. E., Martin, P., Lépine, J. R. D., 2004, A&A, 413, 159

Babusiaux, C., Gilmore, G., 2005, MNRAS, 358, 1309

Babusiaux, C., et al., 2010, A&A, 519, 77

Ballero, S. K., Matteucci, F., Origlia, L., Rich, R. M., 2007, A&A, 467, 123

Bekki, K., Tsujimoto, T., 2011, accepted in ApJ (arXiv1105.5864)

Bensby, T., et al., 2010, A&A, 512, 41

Binney, J., Tremaine, S., 1987 in Galactic Dynamics, Princeton; Princeton Univ. Press.

Chiappini, C.; Matteucci, F., Gratton, R., 1997, ApJ, 477, 765

Combes, F., Sanders, R. H., 1981, A&A, 96, 164

De Propris, R., et al., 2011, ApJ, 732, L36

Dwek, E., et al., 1995, ApJ, 445, 716

Freeman, K. C., 1970, ApJ, 160, 811

Frogel, J. A., Tiede, G. P., Kuchinski, L. E., 2000, AJ, 117, 2296

Fulbright, J. P., McWilliam, A., Rich, R. M., 2006, ApJ, 636, 821

Fulbright, J. P., McWilliam, A., Rich, R. M., 2007, ApJ, $661,\,1152$

Fux, R., 1998, A&A, 327, 983

Gilmore, G., Reid, N., 1983, MNRAS, 202, 1025

Howard, C. D., et al., 2009, ApJ, 702, L153

Johnson, C. I., Rich, R. M., Fulbright, J. P., Valenti, E., McWilliam, A., 2011, ApJ, 732, 108

Meléndez, J., et al., 2008, A&A, 484, L21

Minniti, D., Olszewski, E. W., Liebert, J., White, S. D. M., Hill, J. M., Irwin, M. J., 1995, MNRAS, 277, 1293

Mould, J. R., 1984, PASP, 96, 773

Navarro, J. F., Frenk, C. S., White, S. D. M., 1996, ApJ, 462, 563

Rattenbury, N. J., Mao, S., Sumi, T., Smith, M. C., 2007, MNRAS, 378, 1064

Rich, R. M., Origlia, L., 2005, ApJ, 634, 1293

Ryde, N., et al., 2010, A&A, 509, 20

Shen, J., Rich, R. M., Kormendy, J., Howard, C. D., De Propris, R., Kunder, A., 2010, ApJ, 720, L72

Sugimoto, D., Chikada, Y., Makino, J., Ito, T., Ebisuzaki, T., Umemura, M., 1990, Nat, 345, 33

Tsujimoto T., Bland-Hawthorn J., Freeman K. C., 2010, PASJ, 62, 447

Zoccali, M., et al. 2008, A&A, 486, 177